Use of Aerial Thermal Imaging to Assess Water Status Variability in Hedgerow Olive Orchards

Gregorio Egea[a], Carmen M. Padilla-Díaz[b], Jorge Martínez[a], José E. Fernández[b], Manuel Pérez-Ruiz[a*]

[a] Aeroespace Engineering and Fluid Mechanics Department. University of Seville, Seville 41013, Spain.

[b] Irrigation and Crop Ecophysiology Group, Instituto de Recursos Naturales y Agrobiología de Sevilla (IRNAS, CSIC), Avenida Reina Mercedes 10, 41012, Seville, Spain.

* Corresponding author. Email: manuelperez@us.es

Abstract

Characterization of the spatial variability in tree water status is a prerequisite to conduct precise irrigation management within an orchard. This study assessed the suitability of a crop water stress index (CWSI) derived from high-resolution aerial thermal imagery to estimate tree water status variability in super high density (SHD) olive orchards. The experiment was conducted at a commercial SHD olive orchard near Seville (southwestern Spain). The drip irrigated trees were submitted to three irrigation regimes (four plots per treatment): a full irrigation treatment replacing the crop water needs (ETc) and two regulated deficit irrigation treatments replacing ca. 45% of ETc. During the irrigation season, meteorological variables, soil moisture content, leaf water potential and leaf gas exchange measurements were performed. Infrared temperature sensors (IRTS) installed about 1 m above the canopies were used to derive the required baselines for CWSI calculation. A thermal camera installed on a mini RPAS (Remote Piloted Aerial System) allowed recording high-resolution thermal images at 5 representative dates of the olive tree growing season. CWSI values derived from aerial thermal imagery were sensitive to the deliberately imposed variations in tree water status within the SHD olive orchard. Maximum stomatal conductance and midday stem water potential showed tight correlations with CWSI. We conclude that high resolution thermal imagery captured from a mini RPAS has proven to be a suitable tool to capture tree water status variability within SHD olive orchards.

Keywords: CWSI, precision irrigation, *Olea europaea*, soil water content, spatial variability, transpiration.

1. Introduction

Hedgerow orchards with high planting densities, also called super high density (SHD) olive orchards (1500 to 2000 trees ha^{-1}), are growing exponentially since they were introduced in Spain in the early 1990's. Presently, it is estimated that the area devoted to SHD olive orchards worldwide is over 100,000 ha, of which around half are found in Spain (Rius and Lacarte, 2010). The majority of SHD olive orchards are drip irrigated and, given their growing importance in both devoted land and water use, the development of precision irrigation techniques to increase water use efficiency and crop productivity are needed. An important limitation for efficient irrigation is the spatial variability in crop water requirements since, when water is applied uniformly across the olive orchard, there will be zones unintendedly overwatered and others suffering of soil water deficit. Characterization of the spatial variability in tree water status is therefore a prerequisite to conduct precise irrigation management within SHD olive orchards.

Mapping spatial variability in tree water status with traditional measurements of leaf or stem water potential using a pressure chamber is time consuming and costly. Moreover, this method has also the limitation of the long time required to characterize large orchards, as variations in tree water status due to changes in the atmospheric conditions may mask the actual spatial variability in tree water status. Remote sensing techniques offer a promising alternative to traditional tree water status measurements, as they may provide a snapshot of the whole orchard in a reduced period of time. The advent of Remote Piloted Aerial Systems (RPAS) has opened the possibility to develop remote sensing-based methodologies for precision irrigation more affordably than the costly airborne campaigns with manned aircrafts and with higher spatial and temporal resolutions than those normally offered by satellites.

The use of crop temperature measurements for detecting plant water status was proposed in the 1960s (Fuchs and Tanner, 1966), although it was not until the 1980s when the concept of the crop water stress index (CWSI) was developed (Idso et al. 1981, Jackson et al. 1981). CWSI is a plant water status indicator derived from canopy temperature that has been successfully used since the 1980s, in most cases using hand-held infrared thermometers (Abdullah Alderfasi and Nielsen, 2001). Nowadays, the combined used of modern high-resolution thermal infrared cameras and RPAS offers the possibility to map spatial variability in tree water status from thermal imaging and temperature-derived indicators (Bellvert et al., 2016). CWSI is a normalized index that was developed to overcome the influence that other environmental variables causes on the relationship between crop temperature and water stress (Idso et al. 1981). As reviewed in Maes and Steppe (2012), CWSI can be determined by at least three different methodologies. The empirical CWSI is calculated as Idso et al. (1981):

$$CWSI = \frac{(T_c - T_a) - (T_c - T_a)_{LL}}{(T_c - T_a)_{UL} - (T_c - T_a)_{LL}} \quad \text{(Eq. 1)}$$

where T_c-T_a denotes the measured canopy-air temperature difference; $(T_c$-$T_a)_{LL}$ is the lower limit of $(T_c$-$T_a)$ for a given vapor pressure deficit (VPD) which is equivalent to a canopy transpiring at the potential rate; and $(T_c$-$T_a)_{UL}$ is the maximum $(T_c$-$T_a)$, which corresponds to a non-transpiring canopy. $(T_c$-$T_a)_{LL}$ is a linear function of VPD (non-water-stressed baseline, NWSB) that, once empirically obtained, $(T_c$-$T_a)_{LL}$ is calculated solving the baseline equation for the actual VPD. Based on the above, the objectives of this study were to determine the NWSBs required to compute CWSI in SHD olive orchards, and to assess the suitability of CWSI derived from high resolution aerial thermal imagery to estimate tree water status in SHD olive orchards.

2. Materials and Methods

2.1. Experimental site

The experiment was conducted in 2015 at a commercial SHD olive orchard near Seville, southwestern Spain (37º 15' N, 5º 48' W). The 9-year-old olive trees (*Olea europaea* L., cv. Arbequina) were planted at 4 m x 1.5 m tree spacing (1667 trees ha^{-1}). The drip irrigation system consisted of one drip line per tree row and three 2 L h^{-1} pressure compensating drippers (0.5 m apart) per tree. One flow meter per irrigation treatment recorded the amount of water applied in each irrigation event. An irrigation controller (Agronic 2000, Sistemes Electrònics PROGRÉS, S.A., Lleida, Spain) was used for irrigation scheduling. Trees were fertigated following current commercial practices and no weeds were allowed to grow in the inter row spacing over the spring-summer seasons.

Climate of the study area is Mediterranean, with rainfall occurring normally from late September to May. Average annual data of potential reference evapotranspiration (ET_0) and precipitation recorded over the period 2002-2014 in a standard weather station located near the orchard are 1528 mm and 540 mm, respectively. Table 1 shows the weather data (monthly averages) recorded over the experimental year. The orchard soil has a sandy loam top layer (0.0-0.4 m) and a sandy clay layer (0.4-1.0 m) underneath. The electrical conductivity of the saturated soil-paste (ECe), pH and organic matter content determined for the top soil layer (0.0-0.4 m) was 2.5 dS m^{-1}, 6.34 and 0.28%, respectively.

Table 1. Weather variables measured over 2015 at a nearby standard weather station belonging to the Agroclimatic Information Network of the Junta of Andalusia. *P* (mm): rainfall; *T* (ºC): air temperature; *RH* (%): relative humidity; *u* (m s^{-1}): wind speed; R_s (MJ m^{-2} d^{-1}): solar radiation; ET_0 (mm d^{-1}): FAO-Penman Monteith reference crop evapotranspiration. The suffixes av, mx and mn indicate average, maximum and minimum, respectively.

Month	*P*	T_{av}	T_{mx}	T_{mn}	RH_{av}	RH_{mx}	RH_{mn}	*u*	R_s	ET_0
Jan	42.2	8.8	16.0	2.8	82	99	50	2.3	10.3	1.5
Feb	6.8	9.4	15.8	3.4	75	95	45	2.5	12.5	2.1
Mar	42.0	12.8	21.1	5.2	73	95	40	1.7	18.2	3.1
Apr	26.8	16.4	24.0	9.3	71	97	38	1.6	21.5	4.0
May	0.4	21.6	31.4	11.9	50	86	20	1.6	27.6	6.2
Jun	2.2	24.0	32.8	14.8	47	77	23	2.4	28.5	7.3
Jul	0.0	28.1	37.4	18.6	42	66	17	2.6	29.9	8.9
Aug	1.6	26.1	34.3	18.7	50	73	26	2.6	23.6	7.0
Sep	28.6	21.7	29.4	14.8	59	83	31	2.6	20.4	5.2
Oct	73.4	18.7	25.0	13.7	74	92	45	1.9	12.6	2.9
Nov	33.0	13.7	22.1	7.0	68	91	39	1.7	12.5	2.1
Dec	25.2	12.0	20.3	5.5	70	90	42	1.3	9.1	1.6
Year	282.2	17.8	25.8	10.5	63	87	35	2.1	18.9	4.3

2.2. Irrigation treatments

Three irrigation treatments were imposed in the orchard, as described in Padilla-Díaz et al. (2016). A full irrigation treatment (FI) in which trees were daily irrigated for the whole irrigation season to replace 100% of the irrigation needs (IN) was established. Two regulated deficit irrigation treatments (45RDI) for which the total water supplied along the season was aimed to replace 45% of IN were also established. One of the 45RDI treatments was scheduled on the basis of the crop coefficient method ($45RDI_{CC}$), whereas the other 45RDI treatment was scheduled from outputs of leaf turgor-pressure ($45RDI_{TP}$) or ZIM probes (Zimmermann et al., 2008). More details on the irrigation scheduling and the 45RDI strategies can be found in Padilla-Díaz et al. (2016). A randomized block design with four 12 m × 6 m plots per treatment was used (Fig. 1). Each plot contained 24 trees, and measurements were made in the central 8 trees to avoid border effects.

2.3. Thermal imagery acquisition

A thermal infrared (TIR) camera (Tau 2 324, FLIR Systems, Inc., Oregon, USA) was mounted on a multirotor type of RPAS (Remote Piloted Aerial System) model Phantom 2 (SZ DJI Technology Co., Ltd., Shenzhen, China). The RPAS is equipped with a GNSS receptor, has a flight autonomy of 25 min and a remote control range of 1,000 m in open spaces. The TIR camera was installed aiming vertically downward (nadir view) at the bottom of the RPAS. The camera spectral range is 7.5–13.5 µm with a resolution of 324 x 256 pixels, a focal length of 9 mm, and a field of view of 49° (H) x 39° (V). The thermal images were stored on board in a raw format with 14-bit radiometric resolution and calibrated using known surface temperatures of ground targets collected at the flight time. In particular, temperature of four selected trees measured with four infrared thermometers (IRTS) (see section 2.4), a cold reference (wet cotton sheet) and hot references (40 x 50 cm black plastic panels) located in the centre of each experimental plot (Fig. 1), both measured with a hand-held infrared thermometer model FLUKE 62 Max (FLUKE, Washington, DC, USA), were used as ground targets. The RPAS was flown across the experimental orchard on five clear sky days at 20 m above the ground level and at solar noon, delivering thermal images with a ground spatial resolution of 5 cm.

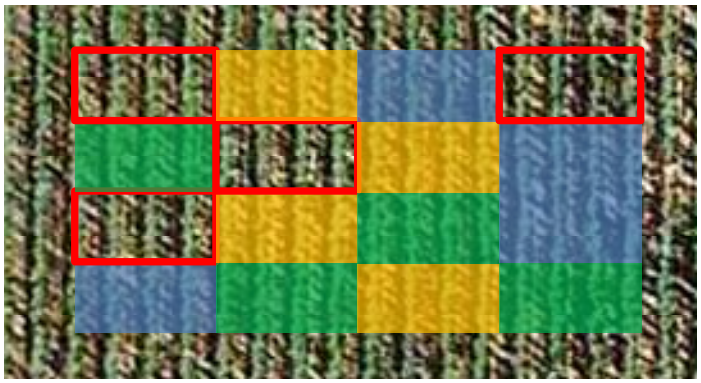

Figure 1. Irrigation treatments distribution in the experimental SHD orchard. FI: blue plots; $45RDI_{CC}$: green plots; $45RDI_{TP}$: yellow plots. The red line rectangles represent plots irrigated following the farmer criteria.

2.4. Measurements at ground level

Volumetric soil water content (θ) was measured in all plots (four per irrigation treatment) with a PR2-type Profile Probe (Delta-T Devices Ltd, Cambridge, UK) at 0.1, 0.2, 0.3, 0.4, 0.6 and 1.0 m depths all along the irrigation season. θ measurements were always performed after irrigation, between 10.00 and 12.00 Greenwich Mean Time (GMT), which is close to solar time at the longitude of our experimental site. The probe was calibrated in situ by Fernández et al. (2011). The θ values were used to calculate changes on the relative extractable water (REW) for all treatments, as described elsewhere (Fernández et al., 2013). Midday stem (Ψ_{st}) water potential was measured with a Scholander-type pressure bomb (PMS Instrument Company, Albany, Oregon, USA) the same days that the RPAS flew. Ψ_{st} was measured at 11:30 – 12:30 GMT in one leaf per tree from two representative trees per plot of each treatment. For Ψ_{st} determination, leaves were taken from the inner part of the canopy, were wrapped in aluminium foil ca. 2 h before measurement. Stomatal conductance (g_s) was measured on the same days and trees where Ψ_{st} was measured, but between 09.00–10.00 GMT, the time for maximum daily stomatal conductance in olive (Fernández et al. 1997). A Licor LI-6400 portable photosynthesis system (Li-cor, Lincoln NE, USA) with a 2 × 3 cm standard chamber was used to measure g_s in sunny leaves of current-year shoots from the outer part of the canopy facing SE and at ambient light (≈ 1,500 µmol m^{-2} s^{-1}) and CO_2 (370 – 400 µmol mol^{-1}) conditions.

Four Infrared Remote Temperature Sensors (IRTs) (model IR120, Campbell Scientific Ltd., Shepshed, UK) were mounted over two representative trees in FI and $45RDI_{TP}$ treatments. The sensors angular field of view is 20º, and the accuracy over calibrated range is ± 0.2 ºC. The IRTS were mounted on galvanized steel masts with an horizontal mounting arm (model IR1X0, Campbell Scientific Ltd., Shepshed, UK) ending with a white PVC solar shield (model IR-SS, Campbell Scientific Ltd., Shepshed, UK) to protect the sensor. The IRTS were mounted aiming vertically downward (nadir view) and targeting the center of the canopy from a distance of approximately 1 m. The dense canopies formed by this type of growing system (i.e. hedgerow olive orchard) allowed IRTS to view mostly foliage in a circular area of approximately 0.35 m of diameter in the canopy top. The IRTS were connected to two dataloggers (model CR1000, Campbell Scientific Ltd., Shepshed, UK) that recorded canopy temperatures (T_c) every minute and stored the 15-min averages. The canopy temperature measurements started on 16 June, 2015 (DOY 167) and continued with a sole interruption of 12 days due to power outage until 5 November (DOY 275).

T_c data measured with the IRTS installed above the well-watered trees were used to derive the Non-Water-Stress Baselines (NWSB) for CWSI calculation. Only clear-sky days were used for NWSB determination. Clear-sky days following a rainfall event were also discarded to avoid errors associated to wet foliage. Air temperature (T_a) along with

VPD data recorded in the weather station at the same time that T_c were used to derive the NWSB of the SHD olive orchard.

2.5. Image processing and CWSI calculation

The thermal images taken with the RPAS were used to calculate the mean canopy temperature (T_c) of each experimental plot. Only the central 8 trees of each plot were used to calculate mean T_c to avoid border effects. An image segmentation algorithm based on the rule of 'full width at half maximum' (FWHM) (Rud et al., 2015) was implemented in R (R Core Team, 2015) to extract pure vegetation pixels from the thermal image. At solar noon, the effects of tree shadow are minimized, and thermal images are composed mainly by canopy, soil and mixed plant-soil pixels. The algorithm allowed distinguishing vegetation from background (mainly soil) according to differences between canopy and soil temperature in each thermal image. Once vegetation pixels were selected from a bi-modal histogram (i.e. histogram with two clearly differentiated peaks ascribed to soil and vegetation pixels in the point cloud) (Figure 2), the FWHM rule was used to distinguish pixels with high probability to be pure vegetation from pixels that are likely to mix vegetation, soil and/or shadow effects. The selected segment was then used to compute mean T_c for each experimental plot. Figure 3 shows an example of the thermal imaging processing carried out.

Mean T_c was used to calculate CWSI for each experimental plot using Eq. 1. For each flight day, ΔT_{LL} was calculated from the NWSB determined with the IRTS as described in section 2.4 and actual air VPD. ΔT_{UL} was determined as T_a + 5ºC based on previous studies dealing with the same crop species (Rud et al., 2015).

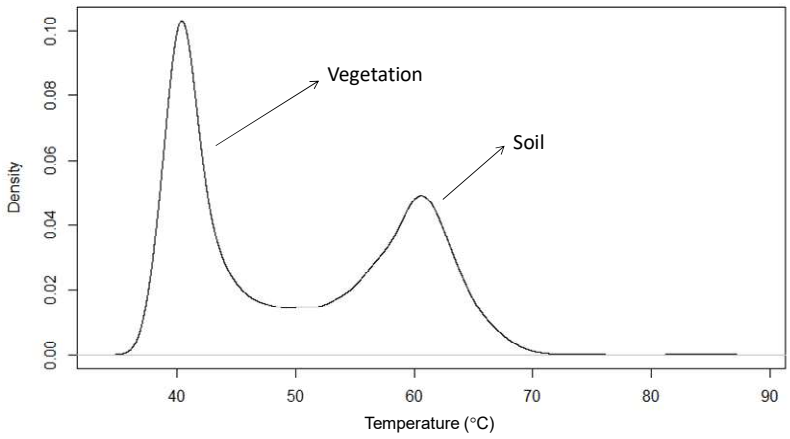

Figure 2. Example of bi-modal histogram of temperatures obtained from a thermal image of an experimental plot.

3. Results and Discussion

3.1. Determination of the non-water stress baselines (NWSB).

The relationship between hourly ΔT (T_c – T_a) and VPD values derived for well-watered olive trees throughout the period of study using clear-sky days did not yield any significant relationship when all hours and days were pooled together (data not shown). The relationships became significant when ΔT and VPD were regressed for a given time of the day, as shown in Figure 4 using data taken at 12.00 GMT. The reason why the relationship ΔT vs VPD for well-watered trees varies diurnally is the influence that weather conditions have on ΔT, as demonstrated theoretically by Maes and Steppe (2012) and confirmed experimentally in previous studies, such as those conducted in pistachio trees (Testi et al., 2008) and vineyard (Bellvert et al., 2014).

In addition to the diurnal effect observed on NWSB, we also observed a marked seasonal variation in the ΔT vs VPD relationship (Figure 4), as the NWSB shifted in August (Period B), as compared to that derived in June-July (Period A), and in September (Period C) as compared to those derived for the Periods A and B. This behaviour was not observed in pistachio trees (Testi et al., 2008), but has also been recently reported for peach trees (Bellvert et al., 2016).

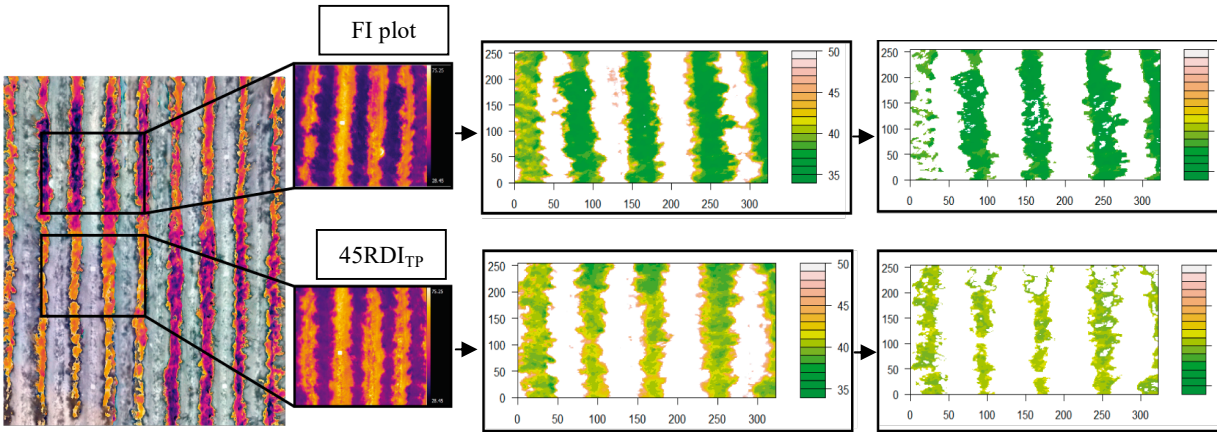

Figure 3. Example of thermal image processing. From left to right: (a) bi-colour thermal mosaic in which part of the temperature range has been selected for highlighting vegetation surface temperatures while the remaining temperature range is shown in grey scale; (b) thermal images of two experimental plots (FI and 45RDI$_{TP}$); (c) thermal images obtained once the vegetation histogram (see Figure 2) has been selected with the segmentation algorithm; (d) thermal images obtained once the FWHM rule has been applied with the segmentation algorithm.

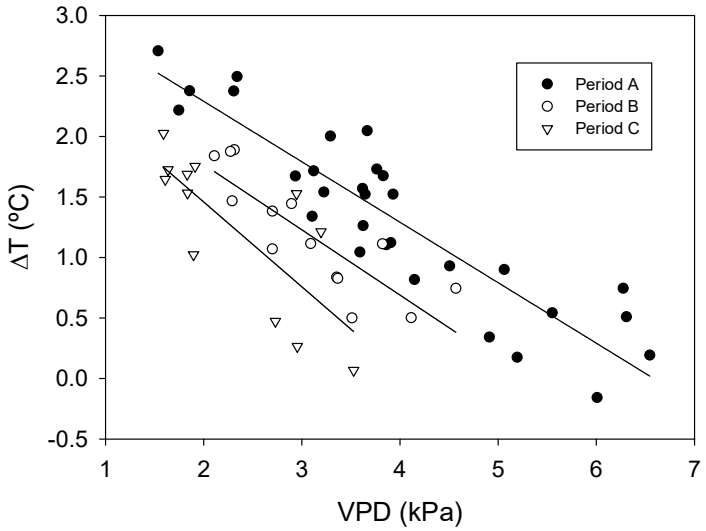

Figure 4. Non-Water Stress Baselines (NWSB: $\Delta T = a + b \cdot VPD$) determined for FI olive trees at solar noon (12.00 GMT). The straight lines represent the regression lines. Period A: June-July, DOY 167-212 ($\Delta T = 3.29 - 0.50 \cdot VPD$, R^2=0.82); Period B: August, DOY 215-243 ($\Delta T = 2.85 - 0.54 \cdot VPD$, R^2=0.71); Period C: September, DOY 244-273 ($\Delta T = 2.86 - 0.70 \cdot VPD$, R^2=0.56). Only clear-sky days were used.

3.2. Seasonal time-course of CWSI

The seasonal time-course of CWSI derived from aerial thermal imaging and the NWSBs described in the previous section showed different trends between the irrigation treatments (Figure 5a). FI trees maintained values close to zero throughout the period of study, which are indicative of non-limiting soil water conditions. The RDI treatments presented mean CWSI values close to those of FI on the first flight day, but their mean CWSI increased up to 0.6-0.7 in the next two flights, coinciding with a period of moderate water restriction in the RDI treatments. From DOY 240 onwards, although differences in CWSI between FI and the RDI treatments were slower, the latter still showed mean CWSI 0.2-0.3 higher than that of FI. No clear differences in CWSI were observed between both irrigation treatments.

The comparison of the seasonal evolutions of CWSI and REW (Figure 5b) reveals certain parallelism among soil water content and CWSI seasonal trends. The period when CWSI was higher in the RDI treatments coincides with the period where REW was lower (i.e. less available soil water) in the RDI treatments, confirming that the CWSI increments observed in the RDI treatments were due to decreased soil water availability.

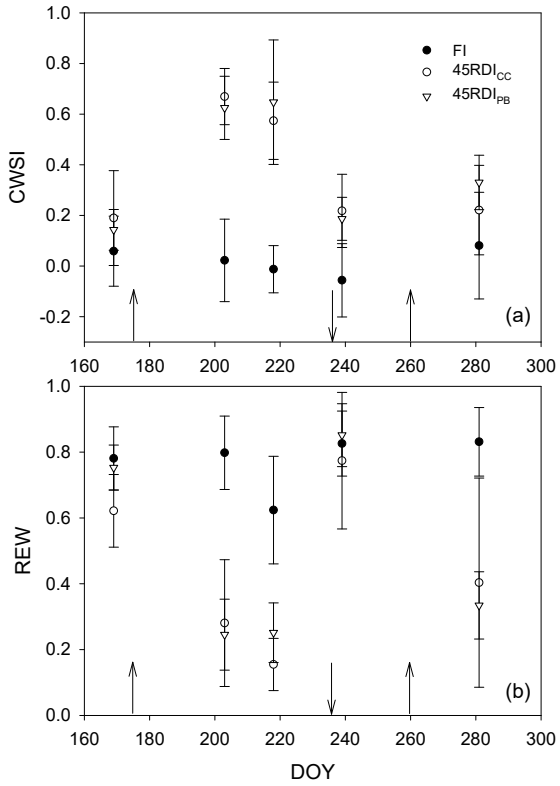

Figure 5. Evolution of (a) CWSI and (b) REW determined for FI, 45RDI$_{CC}$ and 45RDI$_{PB}$ treatments. Each point is the mean of four and three replicates per treatment in (a) and (b), respectively. Up-facing arrows indicate the onset of water stress periods in RDI treatments; the down-facing arrow indicates the end of a water stress period.

3.3. Relationship between CWSI and g_s and Ψ_{st}.

Midday stem water potential (Ψ_{st}) correlated significantly (R^2=0.82) with CWSI across the experimental period (Figure 6a), following a linear relationship irrespective of the phenological stage. In peach trees, Bellvert et al. (2016) observed that the relationship between CWSI and leaf water potential was phenological-stage dependent, following a curvilinear model during the pre-harvest stages and linear during the postharvest stage. In other fruit tree species (pistachio), the CWSI vs Ψ_{st} relationship was also linear and constant for the entire growing season.

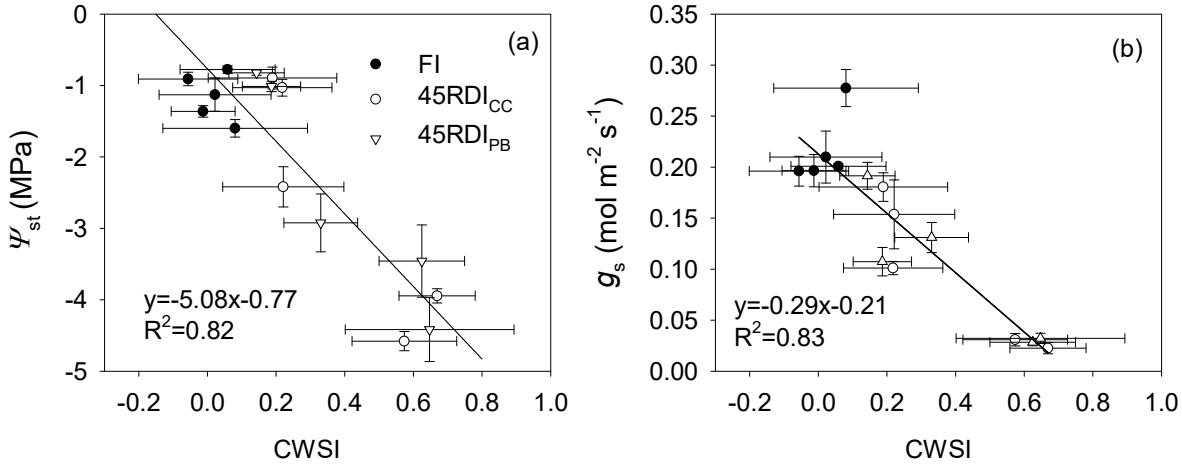

Figure 6. Relationship between CWSI determined from aerial thermal imaging and (a) midday stem water potential (Ψ_{st}) and (b) stomatal conductance (g_s) for FI, 45RDI$_{CC}$ and 45RDI$_{PB}$ treatments. The straight lines represent the fitted regression lines to the data.

When stomata close in response to soil drying, stomatal conductance (g_s) is the physiological parameter that drives canopy temperature increments, as compared to well-watered plants under the same environmental conditions. The relationship between CWSI and g_s derived for the olive trees when all data were pooled together (Figure 6b) was linear and highly significant (R^2=0.83), thus supporting the tight linkage existing between these two water stress indicators. Both g_s and Ψ_{st} showed a similar level of correlation with CWSI, which is explained by the close relationship between g_s and leaf water potential in response to soil drying already observed in olive trees (Erel et al., 2014).

4. Conclusions

This work presents a methodology to infer tree water status variability in SHD olive orchards from remotely sensed thermal imagery captured from a RPAS and Non-Water-Stress Baselines (NWSBs) derived locally for CWSI calculation. The study shows that the segmentation algorithm used, based on bi-modal histogram analysis and the rule of full width at half maximum, allowed extracting pure vegetation pixels from the experimental plots in a heterogeneous crop system such as SHD olive orchards. The NWSBs required for CWSI derivation was not unique throughout the growing season but, in addition to the known diurnal effects, strong seasonal effects were also found. This makes using different equations throughout the growing season to be needed. CWSI showed strong linear relationships with stomatal conductance and stem water potential, demonstrating the promising potential of this method to assessing crop water status variability and supporting irrigation decisions in SHD olive orchards.

Acknowledgements

This work was funded by the Spanish Ministry of Economy and Competitiveness (Project: AGL2012-34544/ECOLIMA) and the Regional Government of Andalucía (Project: P12-AGR-1227). Authors are grateful to Antonio Montero for his valuable contribution in the field work and to the owners of Internacional Olivarera, S.A. (Interoliva), for allowing us to make the experiments in the Sanabria farm.

References

Abdullah Alderfasi, A., D.C. Nielsen, 2001. Use of crop water stress index for monitoring water status and scheduling irrigation in wheat. Agricultural Water Management, 47, 69-75.

Bellvert, J. P.J. Zarco-Tejada, J. Girona, E. Fereres, 2014. Mapping crop water stress index in a “Pinot-noir” vineyard: Comparing ground measurements with thermal remote sensing imagery from an unmanned aerial vehicle. Precision Agriculture, 15, 361–376.

Bellvert, J., J. Marsal, J. Girona, V. Gonzalez-Dugo, E. Fereres, S.L. Ustin, P.J. Zarco-Tejada, 2016. Airborne thermal imagery to detect the seasonal evolution of crop water status in peach, nectarine and Saturn peach orchards. Remote Sensing, 8, 39.

Erel, R., A. Ben-Gal, A. Dag, A. Schwartz, U. Yermiyahu, 2014. Sodium replacement of potassium in physiological processes of olive trees (var. Barnea) as affected by drought. Tree Physiology, 34, 1102-1117.

Fernández, J.E., A. Perez-Martin, J.M. Torres-Ruiz, M.V. Cuevas, C.M. Rodriguez-Dominguez, S. Elsayed-Farag, A. Morales-Sillero, J.M. García, V. Hernandez-Santana, A. Diaz-Espejo, 2013. A regulated deficit irrigation strategy for hedgerow olive orchards with high plant density. Plant and Soil, 372, 279–295.

Fernández, J.E., F. Moreno, I.F. Girón, O.M. Blázquez, 1997. Stomatal control of water use in olive tree leaves. Plant and Soil, 190, 179–192.

Fernández, J.E., F. Moreno, M.J. Martín-Palomo, M.V. Cuevas, J.M. Torres-Ruiz, A. Moriana, 2011. Combining sap flow and trunk diameter measurements to assess water needs in mature olive orchards. Environmental and Experimental Botany, 72, 330–338.

Fuchs, M., C.B. Tanner, 1966. Infrared thermometry of vegetation. Agronomy Journal, 58, 297–601.

Idso, S.B., R.D. Jackson, P.J. Pinter, R.J. Reginato, J.L. Hatfield, 1981. Normalizing the stress-degree day parameter for environmental variability. Agricultural Meteorology, 24, 45–55.

Jackson, R. S. Idso, R. Reginato, P.J. Pinter, 1981. Canopy temperature as a crop water stress indicator. Water Resources Research, 17, 1133–1138.

Maes, W.H., K. Steppe, 2012. Estimating evapotranspiration and drought stress with ground-based thermal remote sensing in agriculture: a review. Journal of Experimental Botany, 63, 4671-4712.

Padilla-Díaz, C.M., C.M. Rodriguez-Dominguez, V. Hernandez-Santana, A. Perez-Martin, J.E. Fernández, 2016. Scheduling regulated deficit irrigation in a hedgerow olive orchard from leaf turgor pressure related measurements. Agricultural Water Management 164, 28–37.

R Core Team (2015). R: A language and environment for statistical computing. R Foundation for Statistical Computing, Vienna, Austria. URL http://www.R-project.org/.

Rius, X., J.M. Lacarte, 2010. La revolución del olivar. El cultivo en seto. Locator Maps PTY. LTD. 518 pp. (In

spanish).

Rud, R., Y. Cohen, V. Alchanatis, I. Beiersdorf, R. Klose, E. Presnov, A. Levi, R. Brikman, N. Agam, A. Dag, A. Ben-Gal, 2015. Characterization of salinity-induced effects in olive trees based on thermal imagery. In Precision Agriculture'15. Wageningen Academic Publishers, Ed. J.V. Stafford. 511-517.

Testi, L., D.A. Goldhamer, F. Iniesta, M. Salinas, 2008. Crop water stress index is a sensitive water stress indicator in pistachio trees. Irrigation Science. 26, 395–405.

Zimmerman, D., R. Reuss, M. Westhoff, P. Geßner, W. Bauer, E. Bamberg, F.W. Bentrup, U. Zimmermann, 2008. A novel, non-invasive, online-monitoring, versatile and easy plant-based probe for measuring leaf water status. Journal of Experimental Botany, 59, 3157–3167.